

Study the Influence of DC Stray Current on the Corrosion of X65 Steel Using Electrochemical Method

Chao Yang, Gan Cui, Zili Li*, Yalei Zhao, Chengbin Zhang

Provincial Key Laboratory of Oil and Gas Storage and Transportation Security, College of Pipeline and Civil Engineering, China University of Petroleum, Qingdao, Shandong, 266580, China

*E-mail: lizili@upc.edu.cn, yangchao201001@163.com.

Received: 3 September 2015 / Accepted: 2 October 2015 / Published: 4 November 2015

The Direct Current (DC) which is generated by HVDC ground electrodes can cause severe corrosion of buried pipelines. In order to explore the influence of DC on the corrosion of pipeline, in this paper, firstly, an electrochemical experimental device was built. Then, according to different DC magnitude, the Tafel curves were tested and the corrosion morphology of the specimens were observed. Our results show that with DC current density increasing, firstly, the corrosion rate increases. However, when the DC density reaches 100 A/m^2 , the corrosion rate decreases because of the formation of the passivation film. And it can be seen by microscope that corrosion product gathers on the surface. With the further increase of the DC density, passivation film dissolves and corrosion product falls off. So corrosion process turns from passivation to action and corrosion rate increases again.

Keywords: Direct current; X65 pipeline steel; Corrosion; DC current density; Polarization curve

1. INTRODUCTION

With the development of society, a lot of alternating current (AC) and direct current(DC) power transmission lines have been built. It is well-known [1,2] that when stray current exists, most metallic materials are corroded at an accelerated rate. Many researchers have studied the effects of AC on metal using simulated or experimental method. Guidance et al.[3] studied the effect of AC on corrosion rate when current densities were lower than 30 A/m^2 . They found that AC current made the corrosion rate accelerate. Fu and Cheng [4] found that AC stray current could result in a decrease of self-corrosion potential of the steel and have an influence on anodic reaction. Xu et al. [5] found that the corrosion rate increased with the AC current density. However, when the AC current density

reached to $600 \text{ A/m}^2 \sim 800 \text{ A/m}^2$, the corrosion rate would decrease, which could be explained by the compact corrosion product layer formed on the steel surface.

In fact, the effect of direct current is much more severe than that of alternating current, especially when high voltage direct current transmission line runs with a single electrode. Nicholson[6] found by testing HVDC(high voltage direct current) fault current can have severe impact on underground/underwater pipelines. This type of DC current flowed into underground pipelines and flowed along the wall of the pipeline for a considerable distance before outflowed. Since HVDC faults are a steady state, the flow of current can last from a few minutes to several days. As a consequence, severe damage can occur to a pipeline at the location where the current outflows. Cui et al. [7] applied BEASY software to study the DC interference corrosion of cathodic system. They considered such influential parameters: soil conductivity, coating damage rate and anodic parameters, et.al. Many researchers [8-10] explored the interference of DC grounding system on buried metal structures and stations. However, the effect of DC stray current on the corrosion potential and corrosion rate has been rare studied.

In order to explore the electrochemical behavior and corrosion surface and describe the changes of corrosion rate and corrosion potential of pipeline steel at various DC, in this work, the study on effect of DC stray current on a pipeline steel was performed by experiment in the solution that is prepared by deionized water and some kinds of ions by polarization technique and morphology of the corrosion surface.

2. EXPERIMENT

2.1 Experimental electrode and solution

In order to explore the effects of DC stray current on pipeline, X65 as a common type of steel was used as the working electrode and the chemical components were shown in Table 1. The size of working electrode is $25 \text{ mm} \times 25 \text{ mm} \times 2 \text{ mm}$ (length \times width \times height). After welding a copper wire on the back surface, using epoxy resin to encapsulate the working electrode. The area of the working electrode is 6.25 cm^2 . The working electrode was disposed by the following process before electrochemical test: Firstly, using #800~1200 waterproof abrasive paper to polish the experimental surface gradually to make the surface mirror-like. Secondly, using acetone and deionized water to clean the experimental surface. At last, using a vacuum drying oven to dry the sample[11]. The whole experiment was performed in solution containing different kinds of ions that take an important role in soil corrosion to replace soil, shown in Table 2.

Table 1. Chemical components of X65 (%)

C	Si	Mn	P	S	Ni	Cu	Mo	N	Nb	Al	Ti	Fe
0.03	0.17	1.51	0.024	0.005	0.17	0.04	0.16	0.006	0.06	0.02	0.01	97.795

Table 2. Components of simulated soil solution (mol/L)

Cl ⁻	SO ₄ ²⁻	HCO ₃ ⁻
0.1	0.1	0.1

2.2 Electrochemical test

Schematic diagram of the experimental set-up is shown in Fig 1[12,13]. The experimental set-up comprises two basic units, which are DC interference system and electrochemical test system. In the DC interference part, the stable direct current source SS2323 can export different stray current into the solution which cause interfered effect on the working electrode. And in the electrochemical test part, the electrochemical station PARSTAT2273 can test polarization curve (TAFEL) of the working electrode.

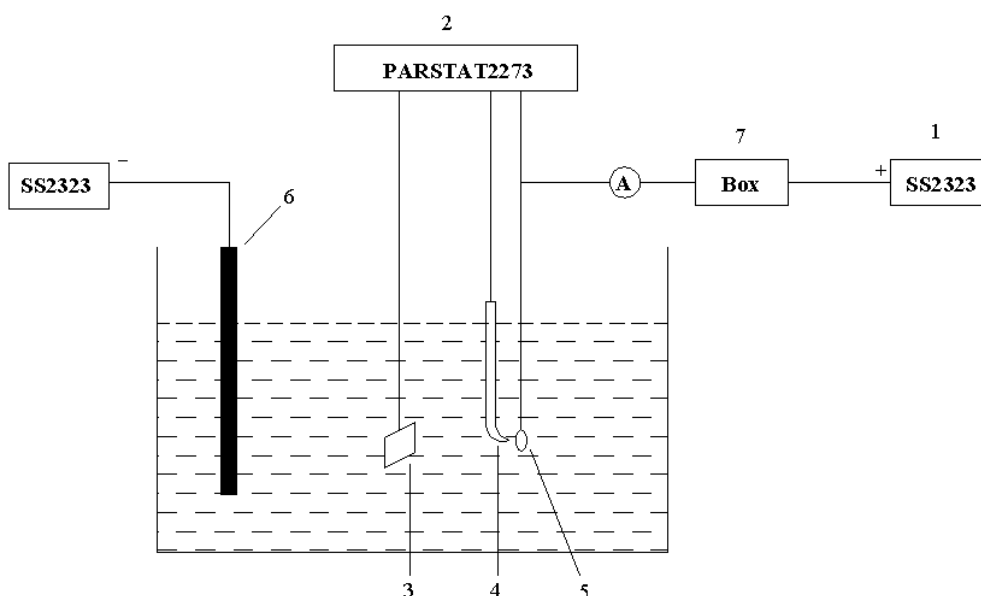


Figure 1. Schematic diagram of the experimental set-up 1-Direct current interference generator 2-Electrochemical station 3-Auxiliary electrode 4-Reference electrode 5-Working electrode 6-Carbon electrode 7-Resistor box

The working electrode is X65 steel. The reference electrode is SCE and the auxiliary electrode is platinum electrode. The reference electrode was electrically connected with the solution by the Luggin capillary. The distance between the tip of the capillary and working electrode is less than 2 mm.

The TAFEL curve was tested with a scanning rate of 0.3mV/s, and a potential range from -250 mV (vs. open circuit potential) to 250 mV (vs. open circuit potential). All the tests were performed in a constant temperature humidity chamber (GDJS-408). Use a scanning electron microscope to observe the surface morphology of the working electrode before and after corrosion.

3. RESULTS AND DISCUSSION

3.1 Effect of DC interference on TAFEL

As we all know, a balance will be realized between the cathodic and anodic reactions on the surface of working electrode when there is no DC interference. At this circumstance, the potential of working electrode is equal to its corrosion potential, precisely [14]. If DC current outflows from working electrode, the working electrode will be polarized which results in the broken of the balance between electrode reactions. As a consequence, the corrosion potential is altered.

Fig.2 is polarization curves of working electrode measured at various DC current densities. From Fig.2, it is obvious that with the increase of current densities, the anodic and cathodic current densities increased. Furthermore, the increase of DC current densities caused increases of E_{corr} of working electrode overall, and E_{corr} and I_{corr} with DC interference are much larger than that without DC interference. However, E_{corr} at $100A/m^2$ is smaller than that at $70A/m^2$.

The fitting results of the polarization curves are summed up in Table 3, which include the DC current density (i_{DC}), corrosion potential (E_{corr}), corrosion current density (I_{corr}), Tafel slope (β_a, β_c) and the ratio of β_a/β_c . From table 3, the changes of anodic Tafel slope β_a is more severe than cathodic Tafel slope β_c . The Tafel slope ratio ($r=\beta_a/\beta_c$) is larger than 1, which means that when DC current outflows from working electrode, anodic polarization occurs and the corrosion process is always anodic control. When DC density is $100A/m^2$, $r=0.447<1$, so I_{corr} decreases theoretically[13]that matches the value in Table 3.

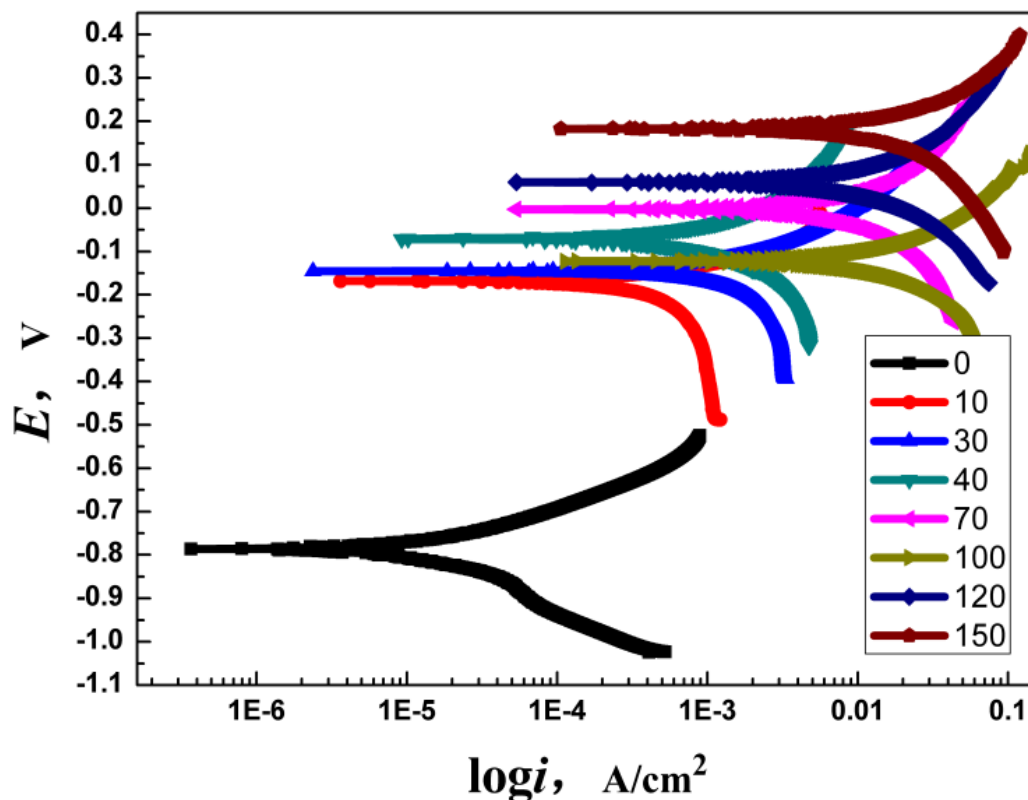


Figure 2. Polarization curves of working electrode at various DC current densities

Table 3. Electrochemical parameters of working electrode at various DC current densities

i_{DC} A/m ²	E_{corr} mV versus SCE	I_{corr} mA/cm ²	β_a mV/decade	β_c mV/decade	β_a/β_c
0	-787.16	0.001508	146.796	107.983	1.359
10	-159.254	8.00	4821.710	227.788	21.168
30	-145.509	22.59	1580.196	224.414	7.041
40	-70.06	35.30	998.782	721.989	1.383
70	-2.46	52.57	1299.392	849.545	1.530
100	-122.311	35.75	665.603	1495.746	0.447
120	-92.699	99.35	1795.035	1023.396	1.754
150	-15.307	93.37	1486.976	1198.968	1.240
200	207.599	120.50	7679.817	627.299	12.243

Fig.3 is the change curves of E_{corr} and I_{corr} of working electrode at various DC current densities. Overall, the increase of DC current densities caused increases of E_{corr} of working electrode. Therefore, under these circumstances, corrosion of the working electrode occurs more easily and the corrosion rate is larger. In theory, when working electrode is anode, E_{corr} should increase with DC current densities [15,16]. However, E_{corr} and I_{corr} decrease at 100A/m².

In order to explore the decreased reason in 100A/m², the scanning range of polarization curve at 70A/m², 100A/m² and 120A/m² was enlarged, as shown in Fig.4. From Fig.4, it is obvious that working electrode is passivated at 100A/m² in the scanning process, while working electrode is not passivated at 70A/m² and 120A/m². Passivation potential E_p is 100.9mV and passivation current density I_{max} is 84.98A/m². Activation potential E_F is 109.3mV and anodic dissolution current density I_p is 15.73A/m². It can be seen that I_{max} is almost equal to i_{DC} .

A passivation film was formed when working electrode was passivated. On the one hand, this film prevents the electronic moving which makes I_{corr} decrease. On the other hand, this film adds resistance of the whole electrode system that makes E_{corr} decrease.

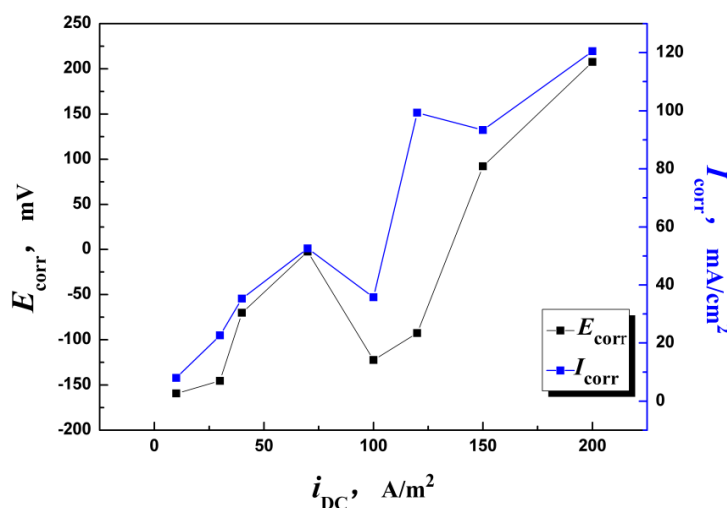


Figure 3. Changes of E_{corr} and I_{corr} of working electrode at various DC current densities

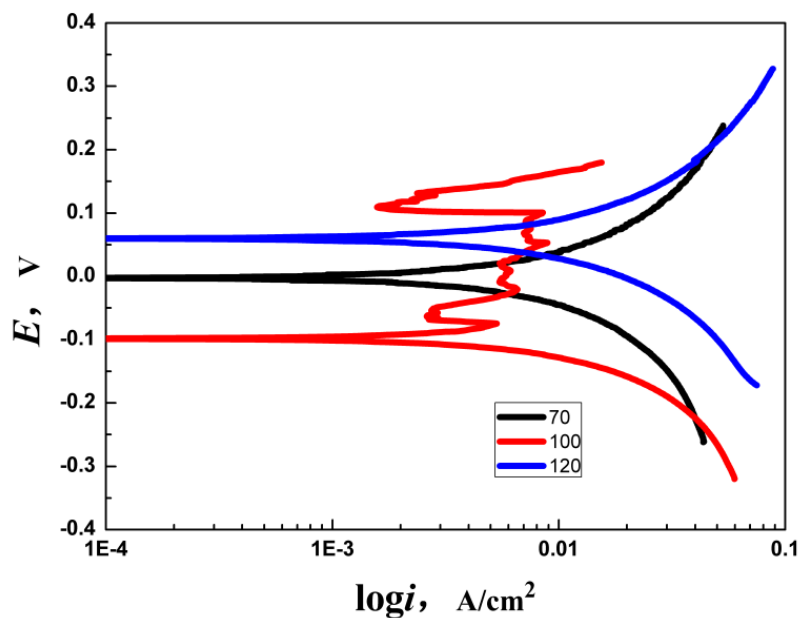
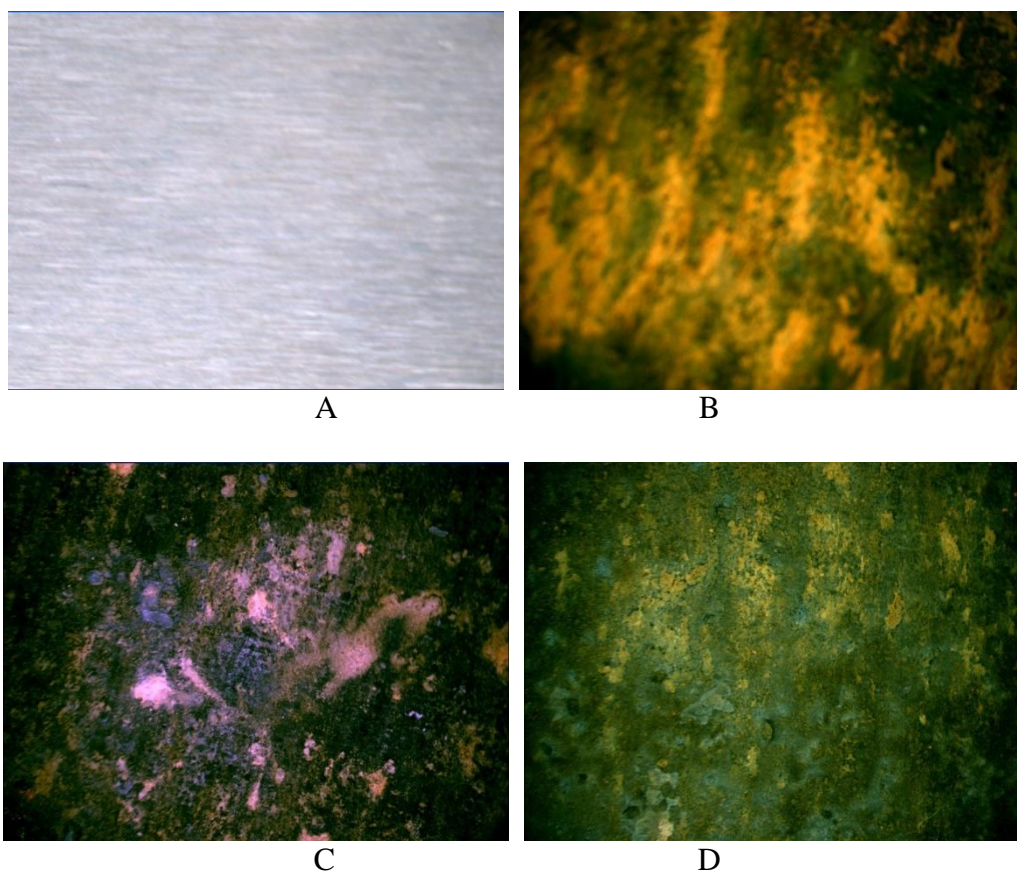


Figure 4. Polarization curve of working electrode at 70A/m², 100A/m² and 120A/m²

3.2 Morphology of the corrosion surface

In this work, use a scanning electron microscope to view the corrosion surfaces before corrosion product was removed.



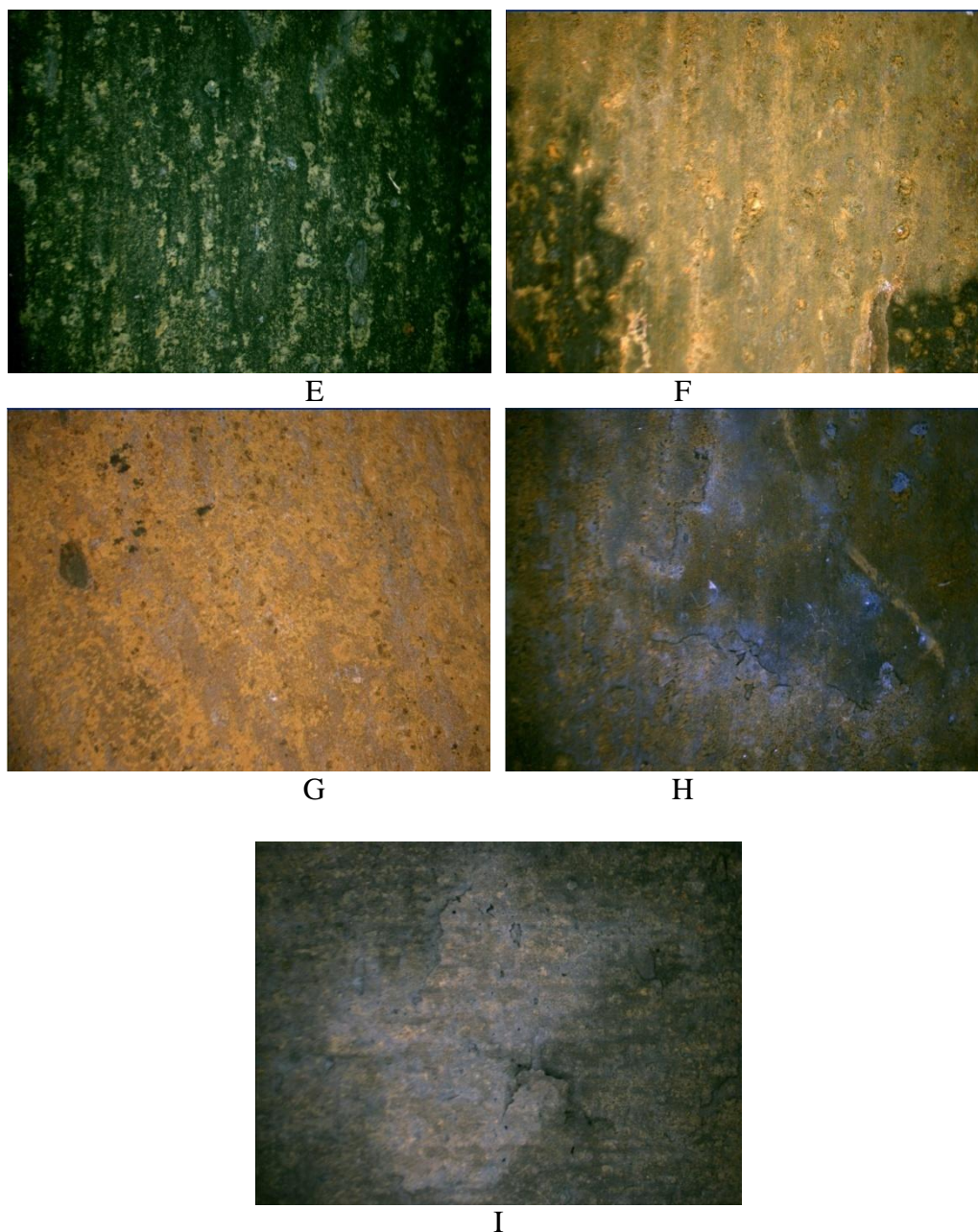


Figure 5. Images of X65 carbon steel electrode at various DC current densities. **A** 0A/m^2 , **B** 10A/m^2 , **C** 30A/m^2 , **D** 40A/m^2 , **E** 70A/m^2 , **F** 100A/m^2 , **G** 120A/m^2 , **H** 150A/m^2 , **I** 200A/m^2 ,

The images of corrosion surfaces were shown in Fig.6. Without DC interference, the working electrode was relatively smooth except for some small corrosion points, as shown in Fig.5(A). When 10A/m^2 DC current density was applied, corrosion became serious and general corrosion occurs on the surface of working electrode, as shown in Fig.5(B). With the DC current densities increase, corrosion became more serious and the corrosion product on the surface accumulated. When DC current density is 100A/m^2 , it is obvious that a corrosion product layer was formed on the surface, as shown in Fig.5(F).

Furthermore, with DC current density increases, corrosion product covering the surface of working electrode fell off and the process turned from dot shedding to exfoliating, as shown in Fig.5(G) and (H). When DC current density increases to 200A/m^2 , only a little corrosion product existed on the surface, as shown in Fig.5(I). the corrosion of working electrode turned from passivation to activation. In the whole process of DC current density increase, the corrosion form is general corrosion.

4. CONCLUSIONS

This work was designed to study effects of DC stray current interference on corrosion of X65 pipeline steel using polarization technique and morphology of corrosion surface, and obtained the following conclusions:

1. Overall, corrosion rate of X65 steel increases with the increase of DC current density, but corrosion rate decreases when DC current density is 100A/m^2 . From polarization curves, it can be seen that X65 steel is passivated at 100A/m^2 that prevents the corrosion. At the same time, corrosion product layer on the surface of X65 steel is formed. Therefore, the corrosion rate decreases. If DC current density continues to increase, the passivation film falls off gradually and X65 steel turns into activation.

2. Corrosion style is general corrosion with DC current. When DC density is smaller than 100mA/m^2 , with DC current density increasing, a uniform corrosion production appears on the surface. However, with the further increase of DC current density, corrosion product covering the surface of working electrode falls off and the process turns from dot shedding to exfoliating.

ACKNOWLEDGEMENTS

This investigation has been performed with the financial support of the Fundamental Research Funds for the Central Universities (No. 15CX06071A).

Reference

1. J.L. Wendt and D-T. Chin. *Corros. Sci.*, 25(1985)889
2. S.B. Lalvani and X. Lin. *Corros. Sci.*, 38(1996)1709
3. S. Goidanich, L. Lazzari and M. Ormellese. *Corros. Sci.*, 52(2010)916
4. A.Q. Fu and Y.F. Cheng. *Corros. Sci.*, 52(2010)612
5. L.Y. Xu, X. Su, Z.X. Yin, Y.H. Tang and Y.F. Cheng. *Corros. Sci.*, 61(2012)215
6. P. Nicholson. Corrosion 2010, Paper No. 10102, NACE, Bolton
7. G. Cui, Z.L. Li, C. Yang and X. Wei. *Corros. Rev.*, 33(2015)233
8. L.G. Liu, M.D. Cui, Z.M. Sun and Y.Q. Chu. *High Voltage Engineering*, 35(2009)1243
9. X.H. Dong, W. Yang, C. Tang and G. Liu. *High Voltage Engineering*, 35(2009)1546
10. S.M. Chen, G.D. Shi, Z.D. Zhao, Z.P. Yu and Z.Y. Qian. *Journal of Zhejiang University*, 27(1993)315
11. H.S. Bi, Z.L. Li, Y.P. Cheng and I. Toku-Gyamerah. *Int. J. Electrochem. Sci.*, 10(2015)
12. Y. Yang, Z.L. Li and C. Wen. *Acta. Metallurgica. Sinica*, 49(2013)43
13. Y.B. Guo, C. Liu, D.G. Wang and S.H. Liu. *Pet. Sci.*, 12(2015)316

14. S. Goidanich , L. Lazzari and M. Ormellese. *Corros. Sci.*, 52(2010)491
15. S. Muralidharan, D.K. Kim, T.H. Ha, J.H. Bae, Y.C. Ha, H.G. Lee and J.D. Scantleburyc. *Desalination*, 216(2007)103
16. S.B. Lalvani and G. Zhang. *Corros. Sci.*, 37(1995)1567

© 2015 The Authors. Published by ESG (www.electrochemsci.org). This article is an open access article distributed under the terms and conditions of the Creative Commons Attribution license (<http://creativecommons.org/licenses/by/4.0/>).